Direct Observation of Plasma-Lens Effect

H. Nakanishi,[1] Y. Yoshida,[2] T. Ueda,[2] T. Kozawa,[2] H. Shibata,[3] K. Nakajima,[1] T. Kurihara,[1] N. Yugami,[4] Y. Nishida,[4] T. Kobayashi,[2] A. Enomoto,[1] T. Oogoe,[1] H. Kobayashi,[1] B. S. Newberger,[1],[a] S. Tagawa,[3] K. Miya,[2] and A. Ogata[1]

[1]*National Laboratory for High Energy Physics, Tsukuba, 305, Japan*

[2]*Nuclear Engineering Research Laboratory, The University of Tokyo, Tokai-mura, Naka-gun, Ibaraki-ken, 319-11, Japan*

[3]*Research Center for Nuclear Science and Technology, The University of Tokyo, Tokai-mura, Naka-gun, Ibaraki-ken, 319-11, Japan*

[4]*Department of Electrical Engineering, Utsunomiya University, Utsunomiya, 321, Japan*

(Received 9 November 1990)

A plasma lens for 18-MeV round-shaped electron beams was experimentally studied; the lens is based on self-focusing due to shielding of the space charge of a particle beam by a quiescent plasma. A differential pumping technique was applied to separate the plasma chamber from the linac acceleration duct. It is shown that the overdense plasmas successfully focus the electron beams. Another finding is that the plasmas appear to reduce the transverse emittance.

PACS numbers: 52.40.Mj, 07.77.+p, 29.25.Fb, 41.80.Ee

A plasma lens based on self-focusing due to shielding of the space charge of a particle beam by a quiescent plasma has been proposed as a final focus device of the next generation of linear colliders.[1,2] Its focusing force can exceed that of a superconducting magnet by several orders of magnitude, since a plasma can support very large electromagnetic fields. This concept is experimentally examined in this paper. Experiments have shown that the plasma certainly has a lens effect, although certain aspects of the results remain unexplained.

There are two regions in a self-focusing plasma lens: overdense and underdense. The physical mechanism of an overdense plasma lens, in which the plasma density is much larger than the beam density, is as follows. In a relativistic electron beam traveling through a vacuum, a repulsive force due to the space charge of all electrons in the bunch is canceled by an attractive force due to a self-magnetic field of the bunch; thus, the beam almost maintains a constant radius. However, if the same beam now enters a plasma, the plasma electrons respond to the excess charge by shifting away from the beam particles. The remaining plasma ions neutralize the space-charge force within the beam; although the plasma is very effective at shielding the space charge of the beam, it is less effective at shielding its current. The beam thus experiences almost the full effect of its self-generated azimuthal magnetic field. In an underdense plasma lens, in which the beam is denser than the plasma, the space charge of the electron beam essentially blows out all of the plasma electrons, leaving a uniform column of positive ion charge.

The experiments were conducted at the Tokyo University 18-MeV linac.[3] It produces a single pulse whose rms length is less than 3 mm, and whose repetition rate is a few Hz. The charge of a pulse was about 0.5 nC. The averaged electron density inside the bunch was about 1.2×10^{10} cm^{-3}. Single-bunch beams were introduced into a plasma chamber, where the plasma density could be varied from the underdense to the overdense region. Transverse profiles of the beams were measured by three phosphor screens placed downstream of the chamber.

We usually separate the plasma chamber from the linac duct using metal foils in order to avoid any vacuum problems. An obstacle to the measurements in this case is multiple scattering of the beam caused by the windows and gas along the beam transport. Differential pumping solves this problem by enabling separation without having to use any hard boundaries. Figure 1 shows the vacuum-line setup. Four turbomolecular pumps were used, three of which were placed between the linac main duct and the plasma chamber. Ducts with low conductance, 16 mm in diameter and 1233 mm in total length, connected the linac and the plasma.

An argon plasma was produced in the chamber, 147 mm in inner diameter and 360 mm in length, by a discharge between the LaB_6 cathodes and the plasma chamber in synchronism with the linac pulse. The plasma pulse width was about 2 msec. It was then confined by the octupole field of permanent magnets placed around the chamber periphery. The magnetic field had a maximum value of 700 G at the chamber wall. One of the features of this confinement is that there is no magnetic field along the beam transport. The plasma density ranged from 0.5×10^{10} to 15×10^{10} cm^{-3} and the temperature from 2.5 to 4 eV, as measured by a Langmuir probe. Measurements of the longitudinal plasma density distribution show that the plasma length along the beam transport is about 150 mm in the case $n_e=1.3\times10^{11}$ cm^{-3}, which increases to 200 mm at $n_e=0.75\times10^{11}$ cm^{-3}. In the radial direction, the homogeneous density region extends to over 50 mm.

Three phosphor screens (Desmarquest AF995R) to

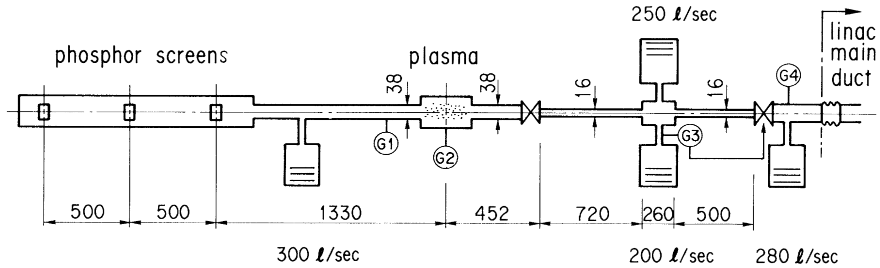

FIG. 1. Vacuum-line setup. Typical pressures measured at gauges G1–G4 without any gas feed are 0.744, 1.43, 0.00957, and 0.0186 mPa, respectively, which change to 38.5, 146, 0.212, and 0.0146 mPa with gas feed, respectively.

measure the profiles were located 1330, 1830, and 2330 mm from the center of the plasma chamber. We call them the first, second, and third screens in this paper, counting from the nearest one to the plasma. Simultaneous measurements using these three screens are impossible because of multiple scattering at the screens. The reproducibility of the linac beams was very good, an important factor in our measurements. The images were observed by a charge-coupled-device (CCD) camera with good linearity, and stored on video tapes and computer processed. The CCD camera was triggered in synchronism with the linac pulse.

Though the experiments spanned both the overdense and underdense regions, we report here only on the overdense case. Also, because it was found that the lens effect of the underdense plasma is roughly proportional to the plasma density, the data have large variances which make quantitative discussion difficult. It was found throughout the experiments that, although the vertical profiles are Gaussian, the horizontal profiles often deviate from Gaussian. The horizontal beam size is always smaller than the vertical beam size, which implies that the beam is horizontally scraped before it reaches the plasma. Figure 2 shows statistical variances, or squares of the standard deviation, of the horizontal and vertical distributions as a function of the plasma density. The figure shows that, first, the beam size is always smallest at the first screen, and increases with distance from the plasma; and, second, the beam sizes decrease as the plasma density increases, except those on the third screen which tend to increase slightly in a high-density region. The three lines in Fig. 2 represent quadratic approximations to the density dependences.

Because there is free space between the plasma and the phosphor screens, it is possible to derive three parameters (two Twiss parameters β and γ, and the emittance) at the plasma as a function of the plasma density from a set of three data at three screens. We have found, however, that real solutions are always obtainable only in the vertical direction. In the horizontal direction, either of the Twiss parameters often becomes imaginary. The solid lines in Fig. 3 show the Twiss parameters and vertical emittance thus calculated. They are related to the beam sizes on the phase-space ellipsoid by the following relations: $\sigma=(\beta\epsilon)^{1/2}$ and $\sigma'=(\gamma\epsilon)^{1/2}$. The emittance and radius in the absence of a plasma are 5.03 mm mrad and 3.72 mm, respectively, which we regard as being the values at the entrance to the plasma.

As Fig. 3 shows, the plasma appears to decrease the emittance. One explanation for the apparent emittance reduction would be beam scraping. However, the density dependence of the total intensity of any screen image eliminates this possibility. If the emittance reduction at the high-density region is due to scraping, the total intensity should decrease. Experimental evidence is to the

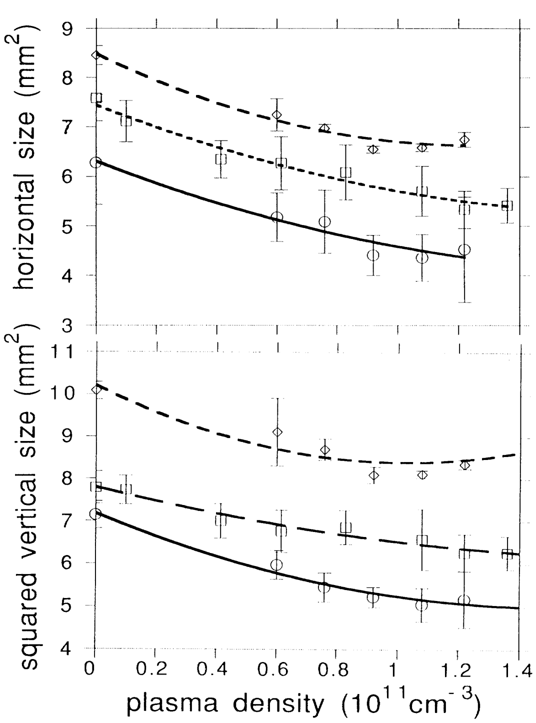

FIG. 2. Variances of the horizontal and vertical distributions observed on three phosphor screens. The solid lines indicate the first screen, the dashed lines the second screen, and the dotted lines the third screen. The error bars were obtained from eighteen pulses of the linac.

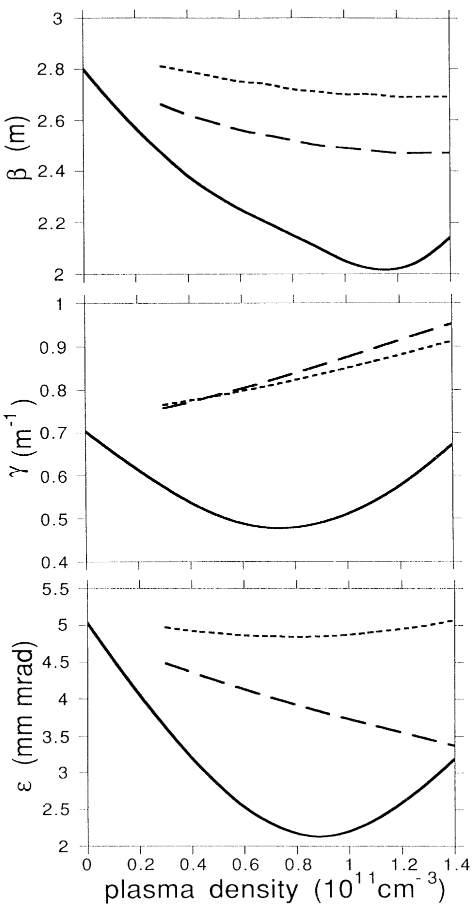

FIG. 3. Dependence of the vertical Twiss parameters and emittance on the plasma density. The solid lines were calculated from the quadratic approximation given in Fig. 2. The dashed lines were calculated based on the assumption that the transverse-emittance decrease is due to a longitudinal-emittance increase. The dotted lines were calculated on the assumption of a constant transverse emittance.

contrary: It is at a minimum in the absence of a plasma, and increases with the plasma density, becoming constant above $n_e > 0.4\times10^{11}$ cm^{-3}. The maximum difference is only 10%. This is probably because the beam spread is so wide without the plasma that the visual field in the computer cannot cover the entire beam region on the screen.

Another plausible explanation would be horizontal-vertical coupling; one may wonder if a decrease in vertical emittance is compensated by the horizontal-emittance growth. Figure 2 eliminates this possibility. We have calculated that a vertical focal point exists just behind the first screen in the absence of a plasma. As the focusing strength increases, the size on the first screen should become smaller, while the size on the third screen should become larger. However, the experimentally obtained vertical size at the third screen does not increase remarkably as the plasma density increases. This is the reason for the apparent emittance reduction. As Fig. 2 shows, the situation is the same in the horizontal direction; in other words, the emittance decrease also takes place in this direction. We must therefore discard the idea of a horizontal-emittance increase.

Another explanation is transverse-longitudinal coupling, in which the transverse-emittance decrease is compensated by a longitudinal-emittance increase. The beam particles experience not only a transverse wake field which causes the lens effect but also a longitudinal wake field which decelerates the particles. The deceleration is null at the head of a beam and maximum at the tail. A substantial energy spread is thus introduced, which increases the area in the longitudinal phase space $(s,\Delta E/E)$. Provided that the total phase-space volume must be conserved, a decrease in transverse-phase-space area or transverse emittance should take place. The dashed line in Fig. 3 shows the emittance thus calculated. The expression for the longitudinal wake field given in Ref. 1 is used to calculate the energy distribution. The resultant distribution is far from Gaussian. The mean energy shift is $\sigma_{\Delta E/E}$ and the bunch length σ_s is assumed to be 3 mm, based on data obtained by a streak-camera measurement. The horizontal-emittance decrease is not taken into account, which may cause the calculated vertical-emittance reduction to be overestimated. As the figure shows, the calculation qualitatively agrees with the experiment.

We now try to explain the density dependence theoretically. In the range $n_e > 0.4\times10^{11}$ cm^{-3}, Chen's conditions of the round-beam limit, $1/4\pi r_e\sigma^2 \gg n_e \gg 4Nk_p^2\sigma_s/\pi\sigma^2$, are satisfied,[1] where the parabolic profiles in both the transverse and longitudinal directions are assumed to be approximations to a Gaussian, with σ and σ_s denoting the bunch radius and half the bunch length, respectively. Under these conditions, the focusing force is linear in r, but proportional to ζ^3: $F = e^2k_p^2N\zeta^3 r/\sigma^2\sigma_l^2$, where ζ denotes the longitudinal position inside a bunch. Using the transfer matrices of free space and the thick lens, and averaging the dependence of the focusing strength on ζ with the weight of a parabolic distribution, we can calculate the beam size at any plasma density.

Let us assume, first of all, that the transverse emittance is independent of the plasma density. The dotted lines in Fig. 4 give the calculated density dependence of the squared sizes at the three screens, where we set the lens length at 150 mm and assume that $\sigma = (\beta_0\epsilon_0)^{1/2} = 3.72$ mm, and $\sigma_s = 3$ mm, with β_0 and ϵ_0 denoting the values in the absence of a plasma. As it shows, the experimental beam sizes are always smaller than those predicted. The dotted lines in Fig. 3 show the dependence of the Twiss parameters and the emittance on the plasma density, calculated from the dotted lines in Fig. 4. It should be noted that the apparent emittance indicates a weak dependence on the plasma density, in spite of the

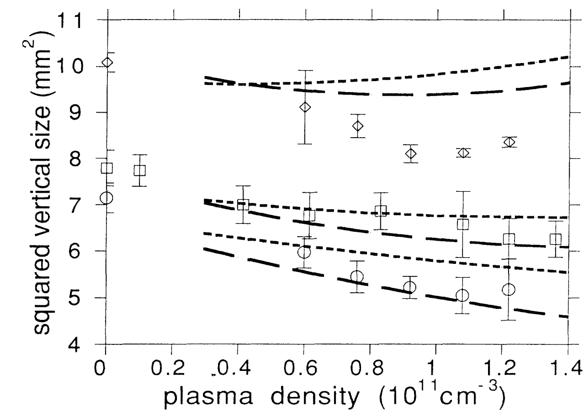

FIG. 4. Theoretical dependences of the squared beam sizes at the three screens on the plasma density. The dotted lines were calculated based on the assumption of the constant transverse emittance, while the dashed lines were calculated based on the assumption that the decrease in the transverse emittance is compensated by an increase in the longitudinal emittance. Experimental data are also given.

fact that the emittance is assumed to be constant.

We next assume that the emittance changes, as shown by the dashed line of Fig. 3. The calculation procedure is simplified as follows: We first assume that a transverse-beam-size reduction takes place, and that the lens is effective for this beam of reduced size. However, an assumption that a beam of reduced size commensurate with the final emittance reduction enters the plasma overestimates the lens effect, because the actual beam-size reduction should be null when a beam enters a plasma and is commensurate with the calculated emittance reduction only when it exits. We therefore average the beam size along the path in the plasma, and assume that a beam with this averaged size enters and that it maintains the size until it exits; specifically, we assume that $\sigma=[\beta_0(\epsilon_0-\Delta\epsilon/2)]^{1/2}$, where $\Delta\epsilon$ is the final emittance reduction. The factor $\frac{1}{2}$ gives the average, since the energy decrease is proportional to the plasma length. The dashed lines in Fig. 4 show the calculated beam size, where the emittance reduction of Fig. 3 is taken into account. They agree with the experimental data better than the dotted lines do. The dashed lines in Fig. 3 show the Twiss parameters, and agreement with the experimental data is poor; still, it is not as bad as that of the dotted lines.

Though our attempt to explain the transverse-emittance decrease in terms of a compensation of the longitudinal emittance gives qualitative agreement with the experimental results, we cannot designate the mechanism which causes the transverse-longitudinal coupling. Simulation results, hitherto reported,[4,5] suggest the existence of such a mechanism. A two-dimensional nonlinear simulation using the parameters of the present experiments is necessary for clarification.

In conclusion, plasma-lens experiments have shown that a plasma has a lens effect. However, beam-size reduction far from the expected focal point is puzzling. We have not as yet conceived of a systematic experimental effect which can explain this observation. On the other hand, transverse-longitudinal coupling explains the observation qualitatively. However, further work is necessary to make this assumption trustworthy; experimentally, longitudinal beam profile measurements and, theoretically, a two-dimensional nonlinear simulation would certainly be helpful in understanding the coupling mechanism.

The authors thank P. Chen, D. Whittum, B. Autin, C. D. Johnson, A. Sessler, and T. Katsouleas for many helpful discussions, and thank P. B. Wilson who suggested the emittance compensation between transverse and longitudinal directions.

[a]Permanent address: University of Texas–Austin, Austin, TX 78712.

[1]P. Chen, Part. Accel. **20**, 171 (1987).

[2]P. Chen, S. Rajagopalan, and J. Rosenzweig, Phys. Rev. D **40**, 923 (1989).

[3]H. Kobayashi and Y. Tabata, Nucl. Instrum. Methods Phys. Res., Sect. B **10/11**, 1004 (1985).

[4]R. Kenigis and M. E. Jones, Phys. Fluids **30**, 252 (1987).

[5]G. Miano, U. De Angelis, and R. Bingham, Plasma Phys. Controlled Fusion **31**, 1381 (1989).